

^{87}Rb NMR study of phase transitions below room temperature in a $\text{LiK}_{0.9}\text{Rb}_{0.1}\text{SO}_4$ mixed crystal

H. J. Kim

*Department of Physics, Korea University, Seoul 136-701, Korea
and Jozef Stefan Institute, University of Ljubljana, Jamova 39, 1000 Ljubljana, Slovenia*

D. Y. Jeong

Department of Physics, Korea University, Seoul 136-701, Korea

B. Zalar and R. Blinc

Jozef Stefan Institute, University of Ljubljana, Jamova 39, 1000 Ljubljana, Slovenia

S. H. Choh*

*Department of Physics, Korea University, Seoul 136-701, Korea
(Received 4 August 1999; revised manuscript received 12 January 2000)*

^{87}Rb NMR spectra in a mixed $\text{LiK}_{0.9}\text{Rb}_{0.1}\text{SO}_4$ single crystal have been investigated in the temperature range from 300 to 80 K. From the electric field gradient analysis, one can suggest that the Rb impurity replaces the K site in the mixed crystal. The temperature dependence of the central NMR frequency of ^{87}Rb ($I = \frac{3}{2}$) demonstrates the phase transition at 255 K which occurs without a change of the Rb^+ site symmetry. In the temperature range from 215 to 176 K, the NMR result shows a mixed phase, our tentative proposal. Another phase transition below 140 K indicates a sudden change in symmetry at the rubidium site in the crystal and a phase transition to a new phase with lower symmetry with the formation of ferroelastic domains. These phase transition temperatures are different from the ^{39}K NMR study in the pure LiKSO_4 and are not in agreement with an optical study in $\text{LiK}_{1-x}\text{Rb}_x\text{SO}_4$ ($x = 0.1, 0.2$). From the angular dependence of the second order quadrupole shift of the central transition of ^{87}Rb NMR, the quadrupole coupling constant and the asymmetry parameter are determined at 300 and 135 K, respectively. The differential scanning calorimeter results clearly show the phase transitions near 257 and 173 K, respectively, but cannot discriminate other phase transitions.

I. INTRODUCTION

An increasing number of studies have been reported on the physical properties of the double sulfate family LiASO_4 , where A is an alkali cation (Li, Na, K, Rb, and Cs). This family shows rather different sequences of the structural phase transitions, which may be related to the dynamics and orientation of the sulfate tetrahedral group in the crystal structure.¹⁻³

LiKSO_4 undergoes several phase transitions in the temperature range from 10 to 1000 K. The exact number of phase transitions and the symmetry of some structural phases, however, are not yet well established. Its crystal structure at room temperature is hexagonal with the space group $C_6^6(P6_3)$ and two formula units per unit cell,⁴ but the structure at the lower temperature phases have been difficult to determine. At room temperature, the potassium ions (K^+) are located on the hexagonal axis and are surrounded by nine oxygen atoms. The sulfate tetrahedra are so distorted that the oxygen atoms at the top may occupy three different sites around the sixfold axis.⁵

The phase transitions of LiKSO_4 at low temperatures have been studied by a variety of methods.⁶⁻¹⁰ However, various results of different experiments are not in accord with each other. This crystal is known to undergo a reconstructive phase transition from the hexagonal $P6_3$ to a trigonal $P31_c$ symmetry around 205 K.^{7,11} Bansal and Roy⁷ proposed that

this phase transition was due to the reorientation of one sulfate group in each unit cell. The crystal structure is illustrated in Fig. 1. The orientations of the tetrahedral sulfate groups in the hexagonal phase are represented by the triangles with solid lines. The trigonal structure differs from the hexagonal one by the rotation of one of the sulfate tetrahedra with dashed lines. Two tetrahedral sulfate groups are displaced from each other by $c/2$ along the crystallographic c axis. The phase transition from the hexagonal $P6_3$ structure to the trigonal $P31_c$ one occurs when one of sulfate tetrahedral groups in each unit cell rotates 108° about one of the axes perpendicular to the c axis.^{7,12}

By further cooling, the LiKSO_4 crystal undergoes another phase transition around 190 K. Once again, there are some controversies with respect to the crystal structure below this phase transition. An orthorhombic structure belonging to the space group $Cmc2_1$ (Ref. 13) and a monoclinic structure belonging to the space group Cc (Ref. 14) were proposed. Kleemann *et al.*¹⁵ have observed a complicated domain superposition below 190 K by means of optical study. Another important feature of this phase transition is the freezing of the orientational disorder resulting in a tilting of the sulfate tetrahedra.^{5,16} Brezowski *et al.* have observed the presence of ferroelastic domains in this phase.¹⁷

EPR measurements of the paramagnetic centers SO_4^- , Cr^{3+} , and Fe^{3+} suggested that the LiKSO_4 crystal has an incommensurate phase between 190 and 295 K in the heating cycle.¹⁸⁻²⁰ Chaplot *et al.*⁶ predicted a possible transition to

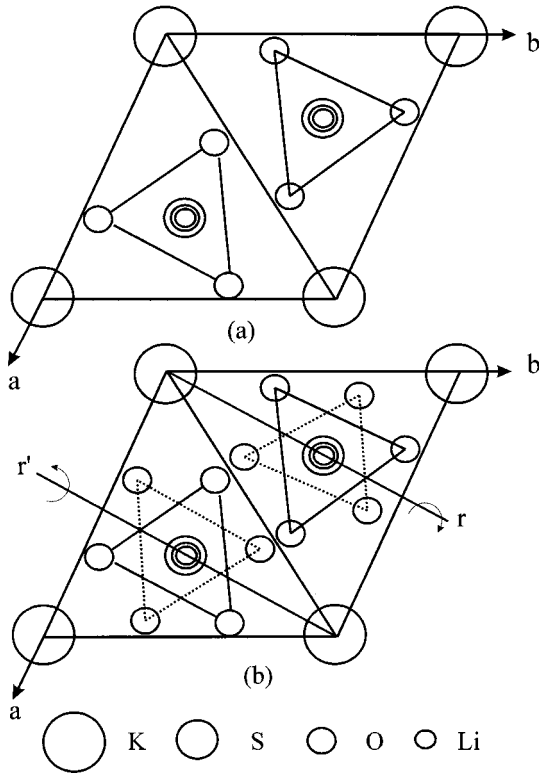


FIG. 1. Crystallographic structure of LiKSO_4 . (a) Hexagonal structure with the $P6_3$ phase at room temperature. (b) Trigonal structure with the $P31_c$ phase. One of tetrahedra of a SO_4^{2-} is rotated about a basal axis (marked r and r') or any equivalent axis.

an incommensurate phase by using the phonon dispersion relation in LiKSO_4 . Perpétuo *et al.*,²¹ however, did not find any evidence of an incommensurate phase at these temperatures by means of EPR of the paramagnetic Ti^{2+} impurity. They found a monoclinic structure below 190 K and twinings within each ferroelastic domain. The ^{39}K NMR study in pure LiKSO_4 (Ref. 14) also did not find any evidence of an incommensurate phase in the same temperature range.

Recently, Moreira *et al.*²² reported the phase transition in the $\text{LiK}_{1-x}\text{Rb}_x\text{SO}_4$ ($x=0.1, 0.2, 0.5$) mixed crystals by means of Raman scattering and birefringence measurements. They observed that the $\text{LiK}_{1-x}\text{Rb}_x\text{SO}_4$ mixed crystals with low rubidium concentration ($x=0.1, 0.2$), though the phase transition temperature was shifted, underwent the same sequence of low-temperature phase transitions as the pure LiKSO_4 compound. The Raman spectra showed that the presence of the Rb ions introduced a local distortion without destroying the long range order of the ionic arrangement. In

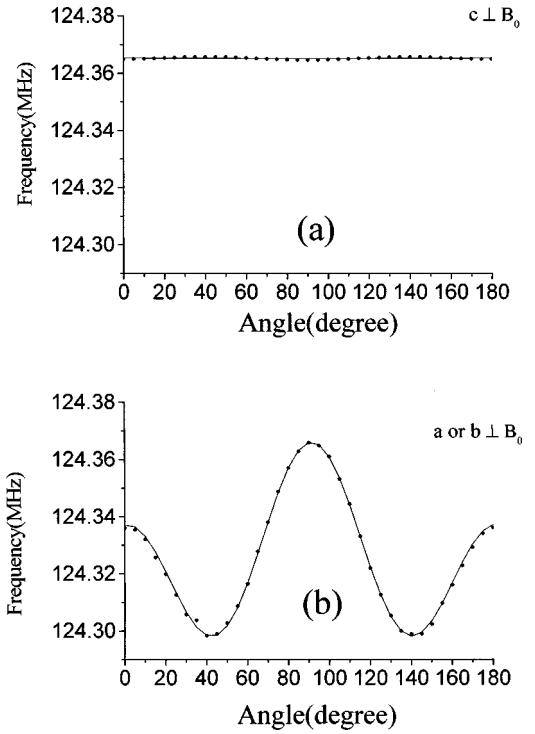


FIG. 2. Angular dependence of the second-order quadrupole shift of the ^{87}Rb NMR central transition ($\frac{1}{2} \rightarrow -\frac{1}{2}$) in the mixed $\text{LiK}_{0.9}\text{Rb}_{0.1}\text{SO}_4$ single crystal (a) for $c \perp B_0$ the shift does not depend on the orientation of the magnetic field with respect to the crystal, and (b) for a or $b \perp B_0$ at room temperature.

order to explain the experimental results, they proposed a qualitative model by assuming that there was a local trigonal distortion due to the Rb ions. They suggested that the ferroelastic transition occurred exactly by breaking the trigonal symmetry due to the occupied Rb ion.

The purpose of this work is to report ^{87}Rb nuclear magnetic resonance (NMR) studies in a $\text{LiK}_{0.9}\text{Rb}_{0.1}\text{SO}_4$ mixed single crystal in the temperature range from 300 to 80 K. The quadrupole coupling constant (e^2qQ/h) and the asymmetry parameter (η) of ^{87}Rb in this crystal are determined at 300 and 135 K, respectively. From the ^{87}Rb NMR results phase transitions are newly proposed in this mixed crystal of $\text{LiK}_{0.9}\text{Rb}_{0.1}\text{SO}_4$ which shows a dramatic change from the pure LiKSO_4 .

II. EXPERIMENTAL PROCEDURES

$\text{LiK}_{0.9}\text{Rb}_{0.1}\text{SO}_4$ single crystals were grown by means of slow evaporation of aqueous solution at 313 K containing the

TABLE I. Comparison of e^2qQ/h , η , and the electric quadrupole moment between ^{87}Rb in $\text{LiK}_{0.9}\text{Rb}_{0.1}\text{SO}_4$ and ^{39}K in LiKSO_4 .

nucleus	$e^2qQ/h_{(\text{exp})}$ (MHz)	η	T (K)	eq_{atomic} (10^{19} V/m ²)	eq_{ionic} (10^{19} V/m ²)	Q	$e^2qQ/h_{(\text{cal})}$ (MHz)
^{39}K	1.270	0	290 ¹⁴	-36.04	6.915	0.060	1.044
	1.470	0.72	180 ¹⁴				
^{87}Rb	7.687	0	300	-69.53	6.915	0.132	6.810
	11.960	0.621	135				

salts $\text{Li}_2\text{SO}_4 \cdot \text{H}_2\text{O}$, K_2SO_4 (90%), and Rb_2SO_4 (10%) in molar ratio. The actual ratio of Rb in $\text{LiK}_{0.9}\text{Rb}_{0.1}\text{SO}_4$ was measured to be 9.4 mol% by means of atomic emission spectrometry (ICP-AES). The crystal axes were determined by using the x-ray diffraction (XRD) method. A single crystal of $\text{LiK}_{0.9}\text{Rb}_{0.1}\text{SO}_4$ of the form of a hexagonal prism with well defined crystal faces was employed in this experiment. Since $\text{LiK}_{0.9}\text{Rb}_{0.1}\text{SO}_4$ crystals were found to be similar to the crystal structure of the pure LiKSO_4 crystal confirmed by our XRD measurements at room temperature, a similar indexing of the crystallographic axes has been used.

Nuclear magnetic resonance spectra of ^{87}Rb ($I=3/2$) in this single crystal were recorded using a Fourier transform NMR spectrometer operating at 9 T produced by a superconducting magnet. The central radio frequency was set at $\nu_0 = 124.373$ MHz for the ^{87}Rb resonance. For the angular dependence of the central transition measured at room temperature and 135 K, respectively, the crystal was rotated around three mutually perpendicular crystal axes a , b , and c , where the c axis being the hexagonal axis at room temperature.

III. RESULTS AND DISCUSSION

A. Quadrupole interaction of ^{87}Rb NMR

The quadrupole perturbed ^{87}Rb NMR spectra can be analyzed by the usual spin Hamiltonian²³

$$H = H_Z + H_Q = -\gamma\hbar\mathbf{B}_0 \cdot \mathbf{I} + \frac{e^2qQ}{4I(2I-1)}(3I_z^2 - I^2) \times \left[\frac{1}{2}(3\cos^2\theta - 1) + \frac{1}{2}\eta\sin^2\theta\cos 2\phi \right] + \text{second order quadrupolar terms} + \dots \quad (1)$$

The angular dependences of the second-order quadrupolar shift for the central NMR line of ^{87}Rb measured at room temperature for rotations around two mutually perpendicular axes are shown in Fig. 2. The experimental values are displayed with dots and the solid lines are obtained by fitting these data to a symmetric second rank EFG tensor. From these results, the nuclear quadrupole coupling constant, $e^2qQ/h = 7.687 \pm 0.002$ MHz, and the asymmetry parameter, $\eta=0$, were obtained. The ^{87}Rb NMR spectrum consists of only one set for all orientations of the applied magnetic field with respect to the crystal. From this fact, it is concluded that all the rubidium sites in the $\text{LiK}_{0.9}\text{Rb}_{0.1}\text{SO}_4$ crystal are magnetically equivalent at room temperature.

The ionic radii of Li^+ , K^+ , and Rb^+ ions are 0.68, 1.33, and 1.49 Å, respectively, and that of $(\text{SO}_4)^{2-}$ is 2.6 Å. In the mixed $\text{LiK}_{0.9}\text{Rb}_{0.1}\text{SO}_4$ crystal, the rubidium ions may only replace the potassium ions and consequently cause a local distortion in the crystal structure due to the substitution.

The quadrupole coupling constant, asymmetry parameter, and electric quadrupole moment of the ^{87}Rb in $\text{LiK}_{0.9}\text{Rb}_{0.1}\text{SO}_4$ and ^{39}K in LiKSO_4 are compared in Table I. It turns out that the quadrupole coupling constant of the ^{87}Rb in $\text{LiK}_{0.9}\text{Rb}_{0.1}\text{SO}_4$ is 6.05 times larger than that of the ^{39}K in LiKSO_4 . Furthermore, Rb and K have the same electronegativity of 0.82. This means that when the Rb impurity replaces the K site in the crystal, the EFG at the resonant nucleus

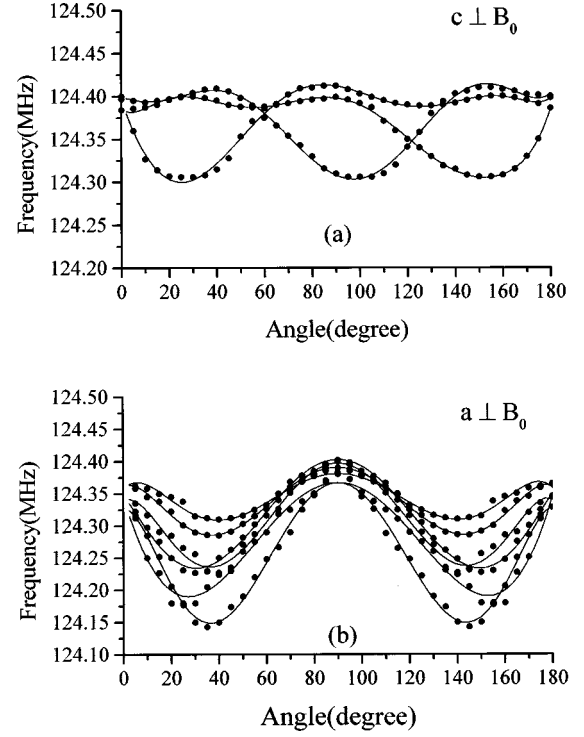


FIG. 3. Angular dependence of the second-order quadrupole shift of the ^{87}Rb NMR central transition ($\frac{1}{2} \rightarrow -\frac{1}{2}$) measured at 135 K in the mixed $\text{LiK}_{0.9}\text{Rb}_{0.1}\text{SO}_4$ single crystal for (a) $c \perp B_0$ and (b) $a \perp B_0$.

depends on the identical ionic contribution around the resonant nucleus. There are two contributions to the electric field gradient; one is the internal atomic contribution due to the electrons surrounding the nucleus and the other is external ionic contribution due to the neighboring ions. This atomic contribution is only from the electron shells of the Rb^+ and K^+ ions and is given by²⁴

$$q_{\text{atomic}} = -\frac{2l}{2l+3} \left\langle \frac{1}{r^3} \right\rangle \quad (2)$$

$$\left\langle \frac{1}{r^3} \right\rangle = \frac{1}{l \left(l + \frac{1}{2} \right) (l+1)} \frac{Z^3}{n^3 a_0^3}, \quad (3)$$

TABLE II. ^{87}Rb electric field gradient tensors in $\text{LiK}_{0.9}\text{Rb}_{0.1}\text{SO}_4$ crystal at 135 K.

(i) 0° domain			
$\frac{eQ}{h} V_{ij}(\text{MHz}) =$	-6.848	3.795	5.928
	3.795	-1.390	3.622
	5.928	3.622	8.256
(ii) 120° domain			
$\frac{eQ}{h} V_{ij}(\text{MHz}) =$	-7.110	-3.280	-6.037
	-3.280	-1.080	3.686
	-6.037	3.686	8.256
(iii) 240° domain			
$\frac{eQ}{h} V_{ij}(\text{MHz}) =$	-6.910	-3.372	6.130
	-3.372	-1.250	-3.561
	6.130	-3.561	8.256

TABLE III. Eigenvalues λ_i (MHz), direction cosines (κ_j) and asymmetry parameter (η) of the ^{87}Rb EFG tensors in $\text{LiK}_{0.9}\text{Rb}_{0.1}\text{SO}_4$ crystal at 135 K.

$\eta = 0.621 \pm 0.004$			
(i) 0° domain			
$\lambda_1 = -2.240 \pm 0.025$	$\lambda_2 = -9.672 \pm 0.055$	$\lambda_3 = 11.960 \pm 0.006$	
	κ_a	κ_b	κ_c
	-0.196	-0.888	0.417
	0.928	-0.315	-0.240
	-0.344	-0.336	-0.877
(ii) 120° domain			
$\lambda_1 = -2.240 \pm 0.025$	$\lambda_2 = -9.672 \pm 0.055$	$\lambda_3 = 11.960 \pm 0.006$	
	κ_a	κ_b	κ_c
	0.126	-0.911	0.393
	0.933	0.243	0.264
	0.336	-0.334	-0.881
(iii) 240° domain			
$\lambda_1 = -2.240 \pm 0.025$	$\lambda_2 = -9.672 \pm 0.055$	$\lambda_3 = 11.960 \pm 0.006$	
	κ_a	κ_b	κ_c
	-0.143	0.909	0.391
	0.928	0.261	-0.226
	0.344	-0.325	0.881

where Z , a_0 , n , and l are the atomic number, the Bohr radius, the principal, and orbital quantum number, respectively. The EFG depends on Z^3 so that heavy atoms will have much larger EFG's than that of the light ones. The neighboring ionic contribution can be expressed by the form²⁴

$$q_{\text{ionic}} = \sum_i Z_{\text{eff}} \frac{3 \cos^2 \theta_k - 1}{r_i^3}, \quad (4)$$

where r_i is the locations of ions with the effective charge Z_{eff} ($= 0.55$ for ^{39}K in LiKSO_4) (Ref. 6) in the lattice. Then the total electric field gradient can formally be expressed by

$$eq = (1 - R)eq_{\text{atomic}} + (1 - \gamma_\infty)eq_{\text{ionic}}, \quad (5)$$

where R and γ_∞ are known as the Sternheimer shielding and antishielding factor ($R^{\text{K}} = 0.438$, $\gamma_\infty^{\text{K}} = -17.32$, $R^{\text{Rb}} = 0.845$, and $\gamma_\infty^{\text{Rb}} = -47.2$).²⁴ From Eq. (5), one may calculate the nuclear quadrupole coupling constant of the ^{87}Rb to be 6.810 MHz and that of ^{39}K to be 1.044 MHz, respectively, as shown in the right hand side of Table I. The calculated EFG value of ^{87}Rb is 6.52 times larger than that of ^{39}K . Although there are substantial uncertainties in the shielding and antishielding factors, it is in fair agreement with the experimental results as summarized in Table I. This result strongly supports the fact that the Rb impurity occupies the K site in the mixed crystal.

At 135 K, well below the phase transition temperatures, the angular dependences of the central NMR line for rotations around two mutually perpendicular crystal axes, a and c are shown in Fig. 3. Dots correspond to the experimental values and the solid lines are obtained by fitting these data to Eq. (1) again. Contrary to the case at room temperature, three sets of NMR lines for the rotation around the c axis and six sets for the a axis were obtained. However, only one set of the quadrupole coupling constant, $e^2qQ/h = 11.960 \pm 0.006$ MHz, and the asymmetry parameter, $\eta = 0.621$

± 0.004 , could be obtained, with the second-order quadrupole effect. This means that though there are 6 physically inequivalent rubidium sites in this phase, all are chemically equivalent. The EFG tensors and eigenvalues are listed in Tables II and III, respectively. From these results, the set of six physically inequivalent ^{87}Rb EFG tensors can be decomposed into three subsets which are related with each other by the 120° rotation around the c axis. Within each subset there are two ^{87}Rb EFG tensors which are related through the c mirror plane and twin domains. In view of the direction cosines, one may notice that the principal axes corresponding to the largest principal values of all these ^{87}Rb EFG tensors are no longer parallel to the hexagonal axis as they are tilted away from the c -axis by approximately 7° about a basal axis. Consequently the threefold symmetry along the c axis is lost. One may conclude that there are three kinds of ferroelastic domains formed at this phase, which is in good agreement with the previous ^{39}K NMR result in pure LiKSO_4 measured at 180 K.¹⁴ The quadrupole coupling constant and the asymmetry parameter of ^{39}K (measured at 180 K) and ^{87}Rb (measured at 135 K) are not exactly in proportion but reasonably comparable as can be seen in Table I.

B. Phase transitions

The temperature dependences of the ^{87}Rb NMR, line shape with the applied magnetic field aligned to the a axis, measured on cooling in the temperature range from 300 to 80 K, are shown in Fig. 4. There is no change in the number of central NMR lines of ^{87}Rb between 300 and 140 K, which includes the I, II, and III phases of LiKSO_4 , namely, the hexagonal, trigonal, and monoclinic phases, respectively. However, the resonance frequency of the central NMR line for ^{87}Rb increases with decreasing temperature as shown in Fig. 5. In addition, there are distinct changes of the ^{87}Rb NMR frequency around 255, 215, 176, and 140 K, respectively.

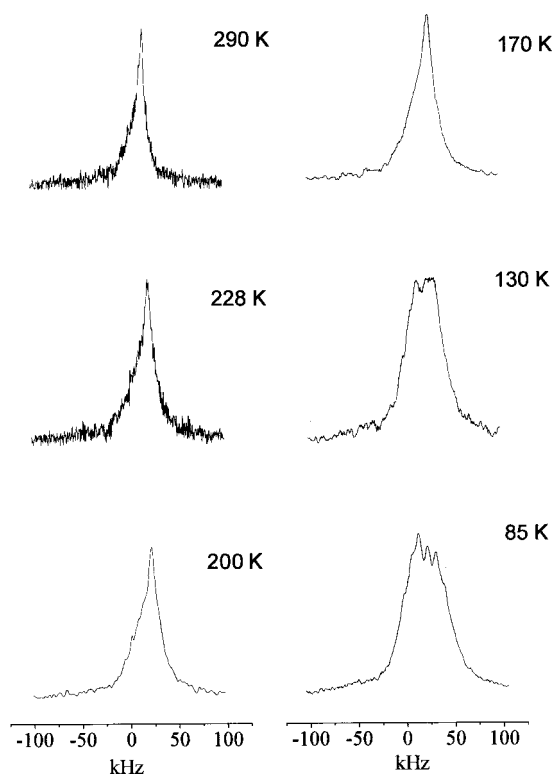


FIG. 4. Temperature dependence of the line shape of the central transition of ^{87}Rb NMR in the temperature range from 300 to 80 K.

At the phase transition around 255 K, $\text{LiK}_{0.9}\text{Rb}_{0.1}\text{SO}_4$ transforms from the hexagonal phase with the space group $P6_3$ to another phase. If there was no disturbance in the long range order of ionic arrangement due to the rubidium impurity, one may assume that the crystal structure in the temperature range from 255 to 215 K may be the trigonal phase as LiKSO_4 . The rubidium ion added in $\text{LiK}_{0.9}\text{Rb}_{0.1}\text{SO}_4$ occupies a greater volume in the unit cell than the potassium ion does due to its larger ionic radius. The presence of the rubidium impurity may cause the shift of the hexagonal-trigonal phase transition from 205 K in the pure LiKSO_4 to 255 K in the mixed crystal.

Below 140 K, the central NMR line is broadened and splits into three lines as displayed in Figs. 4 and 5. This fact

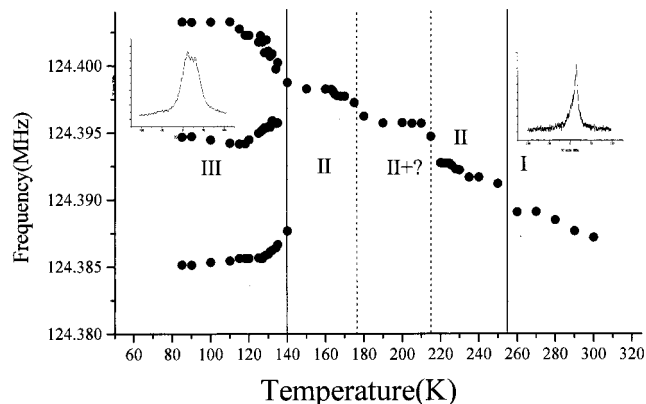


FIG. 5. Temperature dependence of the central ^{87}Rb NMR frequencies in $\text{LiK}_{0.9}\text{Rb}_{0.1}\text{SO}_4$.

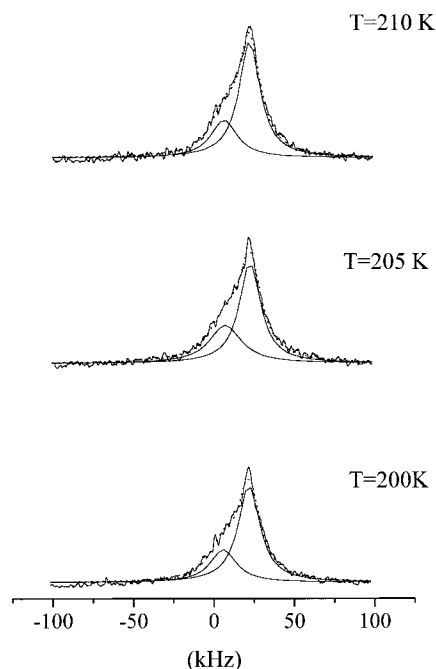


FIG. 6. Comparison of the experimental and best fitted NMR line shape of the central transition of ^{87}Rb in $\text{LiK}_{0.9}\text{Rb}_{0.1}\text{SO}_4$ based on the mixture of hexagonal and trigonal phases. The solid line is the experimental line shape and the dotted line is the best superposed with two Lorentzian curves.

indicates a sudden change in the rubidium site symmetry in the crystal and a phase transition to a new phase with lower symmetry than trigonal. One can suggest that the EFG tensors of spectra of ^{87}Rb at 135 K show the evidence that the crystal structure of $\text{LiK}_{0.9}\text{Rb}_{0.1}\text{SO}_4$ is monoclinic rather than orthorhombic.¹³

The NMR spectra show a possible occurrence of a new phase between 215 and 176 K. To our knowledge, there are no references about this phase, however, one could tentatively propose a possibility of a mixture between the hexagonal and trigonal phases from our NMR spectra. The existence of a mixed phase can be directly inferred from the coexistence of two line shapes indicated in Fig. 6 between 210 and 200 K. Though it is difficult to discriminate two

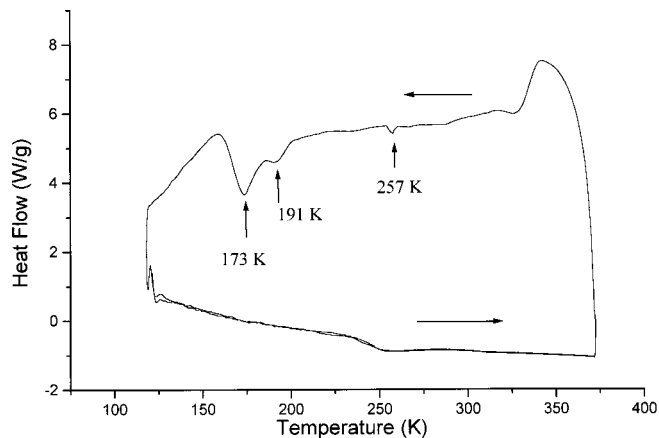


FIG. 7. The DSC results of the heat absorbed and released from a $\text{LiK}_{0.9}\text{Rb}_{0.1}\text{SO}_4$.

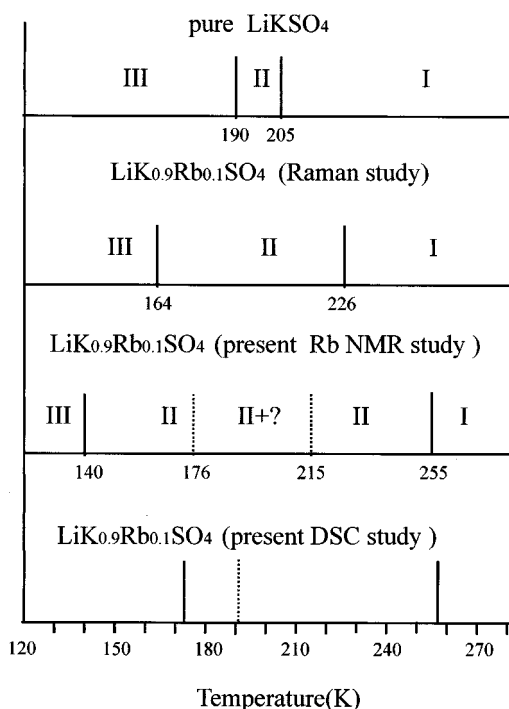


FIG. 8. Comparison of the phase transition scheme between the pure LiKSO_4 , Raman, and the present NMR and DSC studies of $\text{LiK}_{0.9}\text{Rb}_{0.1}\text{SO}_4$ in the temperature range from 300 to 80 K. I, II, and III indicate the hexagonal, trigonal, and monoclinic structure, respectively.

lines, this line shape is best fitted by two Lorentzian curves. The superposed NMR line shape may imply that the hexagonal and trigonal phases may coexist. This mixed phase is not in agreement with the previous Raman result in $\text{LiK}_{1-x}\text{Rb}_x\text{SO}_4$.²² One may consider that the SO_4^{2-} ion orientations in each of these structures are tilted away from the crystal axis about a basal axis but the crystal symmetry is not broken.

The NMR line shape in the temperature range between 176 and 140 K shows the same as that in the trigonal phase. However, when a fraction of potassium ions in the pure LiKSO_4 crystal is replaced by rubidium ions in $\text{LiK}_{0.9}\text{Rb}_{0.1}\text{SO}_4$, the transition temperature is shifted from 190 K in the pure LiKSO_4 down to the lower temperature 140 K in the mixed crystal. The potassium sites may be

considered to be randomly occupied by potassium and rubidium ions with the concentration ratio. Thus, the presence of a small concentration of random rubidium impurities induces a random strain as well as a random fluctuation of the phase at a given nuclear site.

The DSC (differential scanning calorimeter) measurements of the heat absorbed and released from a mixed $\text{LiK}_{0.9}\text{Rb}_{0.1}\text{SO}_4$ crystal were performed (3 °C/min) with a DSC-2010 in the temperature range from 270 to 120 K at Korea Basic Science Institute in Kwangju. The result is displayed in Fig. 7. On cooling, the heat emitted peak appears at about 257, 191, and 173 K, respectively. From NMR and DSC results, one could confirm the existence of first order phase transitions around 255 and 175 K, and higher order phase transitions around 215 and 140 K.

IV. CONCLUSIONS

We have investigated the low temperature phase transitions of the $\text{LiK}_{0.9}\text{Rb}_{0.1}\text{SO}_4$ mixed crystal by means of the ^{87}Rb NMR in the temperature range from 300 to 80 K and DSC from 370 to 120 K. The phase transition temperatures are displayed in Fig. 8 in the investigated temperature range. The presence of discontinuity of the temperature dependence of the ^{87}Rb central NMR frequency associated with the hexagonal to trigonal phase transition at 255 K was clearly demonstrated. It is observed that the mixed crystal may undergo several phase transitions at 255, 215, 175, and 140 K, respectively. The 10% concentration of rubidium in the $\text{LiK}_{0.9}\text{Rb}_{0.1}\text{SO}_4$ causes the shift of the hexagonal-trigonal phase transition to higher temperature by 50 K and the trigonal-monoclinic phase transition to lower temperature by 50 K than that of the pure LiKSO_4 . The ^{87}Rb EFG tensors demonstrate that the crystal structure below 140 K is monoclinic with the formation of ferroelastic domains. Between 215 and 176 K, this crystal exhibits mixed phases due to a deformation of the crystal structure caused by the rubidium ions in the potassium sites.

ACKNOWLEDGMENTS

This work was partially supported by the BSRI program of Ministry of Education (Project No. BSRI-98-2410) in Korea. One of the authors (H.J.K.) is grateful to the Science Foundation of Slovenia.

*Electronic address: shchoh@kucncx.korea.ac.kr

¹H. Z. Cummins, Phys. Rep. **185**, 211 (1990), and references therein.

²A. Desért, A. Gibaud, A. Righi, U. A. Leitão, and R. L. Moreira, J. Phys.: Condens. Matter **7**, 8445 (1995).

³F. Willis, R. G. Leisure, and T. Kanashiro, Phys. Rev. B **54**, 9077 (1996).

⁴A. F. Bradley, Philos. Mag. **49**, 1225 (1925); M. Karppinen, J. O. Lundgren, and R. Liminga, Acta Crystallogr., Sect. C: Cryst. Struct. Commun. **39**, 34 (1983).

⁵P. E. Tomaszewski and K. Lukaszewicz, Phase Transit. **4**, 37 (1983).

⁶S. L. Chaplot, K. R. Rao, and A. P. Roy, Phys. Rev. B **29**, 4747 (1984).

⁷M. L. Bansal and A. P. Roy, Phys. Rev. B **30**, 7307 (1984).

⁸S. Shin, Y. Tezuka, and A. Sugawara, Phys. Rev. B **44**, 11 724 (1991).

⁹R. C. de Sousa, J. A. C. Paiva, J. M. Filho, and A. S. B. Sombra, Solid State Commun. **87**, 959 (1993).

¹⁰U. A. Leitão, A. Righi, P. Bourson, and M. A. Pimenta, Phys. Rev. B **50**, 2754 (1994).

¹¹M. L. Bansal, S. K. Deb, A. P. Roy, and V. C. Shani, Solid State Commun. **36**, 1047 (1980).

¹²M. A. Pimenta, P. Echegut, Y. Luspin, G. Hauret, F. Gervais, and P. Abekard, Phys. Rev. B **39**, 3361 (1989).

¹³R. Cach, P. E. Tomaszewski, and J. Bornarel, J. Phys. C **18**, 915 (1985).

¹⁴B. Topič, U. Haebleren, and R. Blinc, Z. Phys. B: Condens. Mat-

- ter **70**, 95 (1988).
- ¹⁵W. Kleemann, F. G. Schäfer, and A. S. Chaves, *Solid State Commun.* **64**, 1001 (1987).
- ¹⁶S. Bhakay-Tamhane and A. Sequeira, *Ferroelectrics* **69**, 241 (1986).
- ¹⁷T. Braczewski, T. Krajewski, and B. Mr'oz, *Ferroelectrics* **33**, 9 (1981).
- ¹⁸F. Holuj and M. Diozdowski, *Ferroelectrics* **36**, 379 (1981).
- ¹⁹C. H. A. Fonseca, G. M. Riberio, R. Gazzinelli, and A. S. Chaves, *Solid State Commun.* **46**, 22 (1983).
- ²⁰L. Conte and F. Holuj, *Phase Transit.* **6**, 259 (1986).
- ²¹G. J. Perpétuo, M. S. S. Dantas, R. Gazzinelli, and M. A. Pimenta, *Phys. Rev. B* **45**, 5163 (1992).
- ²²R. L. Moreira, P. Bourson, U. A. Leitao, A. Righi, L. C. M. Belo, and M. A. Pimenta, *Phys. Rev. B* **52**, 12 591 (1995).
- ²³A. Abragam, *The Principles of Nuclear Magnetism* (Oxford University Press, Oxford, 1961), Chap. VII.
- ²⁴E. A. C. Lucken, *Nuclear Quadrupole Coupling Constants* (Academic Press, London, 1969), Chap. 4.